

Diffraction gratings of isotropic negative phase-velocity materials

Ricardo Angel Depine ⁽¹⁾ and Akhlesh Lakhtakia⁽²⁾

⁽¹⁾*Grupo de Electromagnetismo Aplicado, Departamento de Física,
Facultad de Ciencias Exactas y Naturales, Universidad de Buenos Aires,
Ciudad Universitaria, Pabellón I, 1428 Buenos Aires, Argentina*

⁽²⁾*Computational & Theoretical Materials Sciences Group (CATMAS),
Department of Engineering Science & Mechanics,
Pennsylvania State University, University Park, PA 16802-6812, USA*

Abstract

Diffraction of electromagnetic plane waves by the gratings made by periodically corrugating the exposed planar boundaries of homogeneous, isotropic, linear dielectric-magnetic half-spaces is examined. The phase velocity vector in the diffracting material can be either co-parallel or anti-parallel to the time-averaged Poynting vector, thereby allowing for the material to be classified as of either the positive or the negative negative phase-velocity (PPV or NPV) type. Three methods used for analyzing dielectric gratings — the Rayleigh-hypothesis method, a perturbative approach, and the C formalism — are extended here to encompass NPV gratings by a careful consideration of field representation inside the refracting half-space. Corrugations of both symmetric as well as asymmetric shapes are studied, as also the diversity of grating response to the linear polarization states of the incident plane wave. The replacement of PPV grating by its NPV analog affects only nonspecular diffraction efficiencies when the corrugations are shallow, and the effect on specular diffraction efficiencies intensifies as the corrugations deepen. Whether the type of the refracting material is NPV or PPV is shown to affect surface wave propagation as well as resonant excitation of surface waves.

PACS numbers: 42.25.Fx, 78.20.Ci

Keywords: grating; negative phase velocity; nonspecular diffraction; numerical techniques; nonspecular diffraction; surface waves

I. INTRODUCTION

Diffraction gratings are not only exploited by nature for the production of color [1] but have also been extensively used in optics for several centuries [2]. During the last century, tremendous progress in manufacturing techniques made diffraction gratings as the spectral dispersive elements of choice. Spectacular progress was also made on the numerical solution of the time-harmonic Maxwell equations for diffraction gratings, thereby greatly facilitating analysis and design [3]. Given such remarkable developments, one would think that the last word on diffraction gratings is imminent; but the emergence of isotropic dielectric-magnetic materials exhibiting phase velocity vector opposed in direction to the time-averaged Poynting vector [4]-[6] has opened new prospects for diffraction gratings.

Typically, a diffraction grating is a slab of either a metal or a dielectric material whose exposed surface is periodically corrugated. When a plane wave is incident on this surface, it is reflected partially in the specular direction fixed by Snel's law [7] and partially in nonspecular directions fixed by the periodicity of the corrugated surface in relation to the free-space wavelength. In addition, specular as well as nonspecular refraction into the slab may also occur, depending on the type of material. Finally, reflections from the back surface also contribute to the overall reflection from the grating, but those need not be considered when examining the essence of the phenomenon of diffraction. As the angle of incidence is changed, specular as well as nonspecular components of the reflected field wax and wane, which phenomenon is technologically exploitable.

What would happen if a diffraction grating were to be made of an isotropic dielectric-magnetic material? If the phase velocity and the time-averaged Poynting vectors in this material are co-parallel, then the effects are not qualitatively different from a diffraction grating made of simply an isotropic dielectric material [8], while the quantitative differences are due to differences in the relative impedance and the wavenumber inside the diffracting material [9]. This paper is devoted to the case when the phase velocity and the time-averaged Poynting vectors in the diffracting material are oppositely directed. Though several names have been proposed for this class of materials, we think that the most descriptive is:

negative phase-velocity (NPV) materials. In contrast, the phase velocity and the time-averaged Poynting vectors are co-parallel in positive phase-velocity (PPV) materials. PPV materials are, of course, commonplace.

The plan of this paper is as follows: The boundary value problem of a diffraction grating is presented in Section II, with careful delineation of field characteristics in the refracting half-space. Three methods of solving the boundary value problem are extended in Section III to encompass NPV refracting materials. These methods are: (i) the Rayleigh-hypothesis method, (ii) perturbative approach, and (iii) the C formalism. Numerical results for corrugations of both symmetric as well as asymmetric shapes are presented in Section IV, and the effects of replacing a PPV material by its NPV analog, or *vice versa*, are extracted from those results. An $\exp(-i\omega t)$ time-dependence is implicit, with $i = \sqrt{-1}$, ω as the angular frequency, and t as the time.

II. BOUNDARY VALUE PROBLEM

In a rectangular coordinate system (x, y, z) , we consider the periodically corrugated boundary $y = g(x) = g(x + d)$ between vacuum and a homogeneous, isotropic, linear, passive, dielectric-magnetic material, with d being the corrugation period. The region $y > g(x)$ is vacuum, whereas the material occupying the region $y < g(x)$ is characterized by complex-valued scalars $\epsilon_2 = \epsilon_{2R} + i\epsilon_{2I}$ and $\mu_2 = \mu_{2R} + i\mu_{2I}$ that depend on ω . If this medium is of the NPV type, then the following three conditions hold equivalently [10, 11]:

$$\left. \begin{aligned} (|\epsilon_2| - \epsilon_{2R})(|\mu_2| - \mu_{2R}) - \epsilon_{2I}\mu_{2I} &> 0 \\ \epsilon_{2R}\mu_{2I} + \epsilon_{2I}\mu_{2R} &< 0 \\ \epsilon_{2R}|\mu_2| + \mu_{2R}|\epsilon_2| &< 0 \end{aligned} \right\}. \quad (1)$$

None of the three conditions hold for a PPV material.

A linearly polarized electromagnetic plane wave is incident on this boundary from the region $y > g(x)$ at an angle θ_0 , ($|\theta_0| < \pi/2$), with respect to the y axis, as shown in Figure 1. This plane wave can be either s -polarized or p -polarized [12]. Given the orientation of the

plane wave with respect to the grating plane (i.e., the xy plane), all reflected and transmitted fields must be linearly polarized in the same way as the incident plane wave [13].

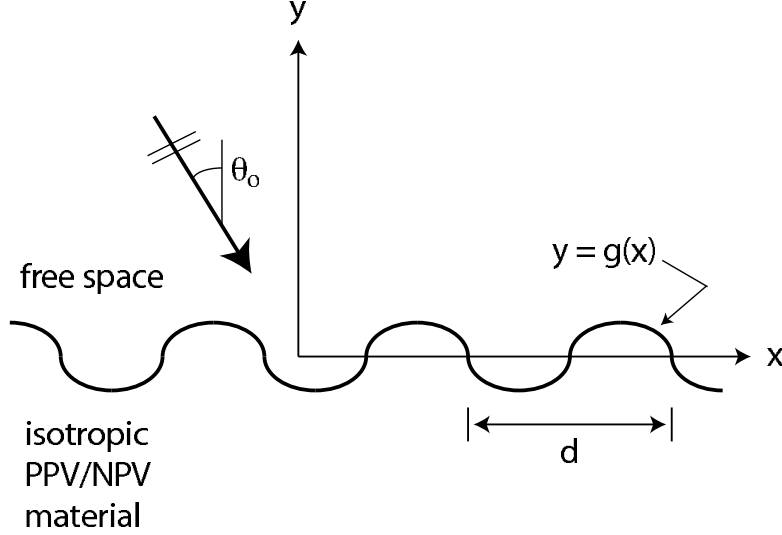


FIG. 1: Schematic of the boundary value problem. A plane wave is incident at an angle θ_0 , ($|\theta_0| < \pi/2$), with respect to the y axis on the periodically corrugated boundary $y = g(x) = g(x+d)$ between free space and a homogeneous, isotropic, linear dielectric–magnetic material.

Let the function $f(x, y)$ represent the z -directed component of the total electric field for the s -polarization case, and the z -directed component of the total magnetic field for the p -polarization case. After starting from the time-harmonic Maxwell equations, this function can be shown to be a solution of the Helmholtz equations

$$\left. \begin{aligned} \left(\nabla^2 + \frac{\omega^2}{c^2} \right) f(x, y) &= 0, & y > g(x) \\ \left(\nabla^2 + \frac{\omega^2}{c^2} \epsilon_2 \mu_2 \right) f(x, y) &= 0, & y < g(x) \end{aligned} \right\}, \quad (2)$$

where c is the speed of light in free space (i.e., vacuum). Outside the corrugation region $\max g(x) > y > \min g(x)$, the field $f(x, y)$ is rigorously represented as a superposition of plane waves as follows:

$$f(x, y) = \begin{cases} \exp \left[i (\alpha_0 x - \beta_0^{(1)} y) \right] + \\ \quad + \sum_{n=-\infty}^{\infty} c_n^{(1)} \exp \left[i (\alpha_n x + \beta_n^{(1)} y) \right], & y > \max g(x) \\ \sum_{n=-\infty}^{\infty} c_n^{(2)} \exp \left[i (\alpha_n x - \beta_n^{(2)} y) \right], & y < \min g(x) \end{cases} . \quad (3)$$

Here, $c_n^{(p)}$, ($-\infty < n < \infty$; $p = 1, 2$), are scalar coefficients to be determined by the solution of a boundary value problem, while

$$\left. \begin{aligned} \alpha_n &= \frac{\omega}{c} \sin \theta_0 + 2n\pi/d \\ \beta_n^{(1)} &= \sqrt{\frac{\omega^2}{c^2} - \alpha_n^2} \\ \beta_n^{(2)} &= \sqrt{\frac{\omega^2}{c^2} \epsilon_2 \mu_2 - \alpha_n^2} \end{aligned} \right\}. \quad (4)$$

Both $\beta_n^{(1)}$ and $\beta_n^{(2)}$ are double-valued functions by virtues of their definitions as square-roots. If $\beta_n^{(p)}$ represents an *upgoing* plane wave, then $-\beta_n^{(p)}$ represents a *downgoing* wave, and *vice versa*. We must choose the correct signs for all $\beta_n^{(1)}$ as upgoing plane waves as well as for all $\beta_n^{(2)}$ as downgoing plane waves. If $\beta_n^{(p)}$ is real-valued, it corresponds to a propagating plane wave; otherwise, it indicates evanescence.

Note that $\beta_n^{(1)}$ is either purely real or purely imaginary; and the condition

$$\left. \begin{aligned} \operatorname{Re} [\beta_n^{(1)}] &\geq 0 \\ \operatorname{Im} [\beta_n^{(1)}] &\geq 0 \end{aligned} \right\} \quad \forall n \quad (5)$$

is appropriate for upgoing plane waves in the vacuous half-space $y > g(x)$. As the direction and/or the angular frequency of the incident plane wave change, $\beta_n^{(1)}$ may change from purely real to purely imaginary, or *vice versa*. Such alterations are usually marked by noticeable discontinuities in the diffraction spectrums and, hence, are called *Rayleigh-Wood anomalies* although their occurrences are not at all anomalous [3].

The refracting half-space $y < g(x)$ being filled by a material medium, $\epsilon_{2I} > 0$ and $\mu_{2I} > 0$ by virtue of causality [14, 15]. The refracted plane waves must attenuate as $y \rightarrow -\infty$, which requirement leads to the condition

$$\operatorname{Im} [\beta_n^{(2)}] > 0 \quad \forall n. \quad (6)$$

This condition on $\operatorname{Im} [\beta_n^{(2)}]$ automatically fixes the sign of $\operatorname{Re} [\beta_n^{(2)}]$, regardless of the signs of ϵ_{2R} and μ_{2R} ; furthermore, the transformation $\{\epsilon_{2R} \rightarrow -\epsilon_{2R}, \mu_{2R} \rightarrow -\mu_{2R}\}$ alters the signs of the real parts of all $\beta_n^{(2)}$.

In order to find the scalar coefficients $c_n^{(p)}$, we must apply the boundary conditions at $y = g(x)$. These conditions, expressing the continuity of the tangential components of the

total electric field and the total magnetic field, can be written as

$$\left. \begin{aligned} f(x, g(x)+) &= f(x, g(x)-) \\ \hat{n} \cdot \nabla f(x, g(x)+) &= \sigma^{-1} \hat{n} \cdot \nabla f(x, g(x)-) \end{aligned} \right\}, \quad (7)$$

where $\sigma = \mu_2$ for the s -polarization case and $\sigma = \epsilon_2$ for the p -polarization case, while \hat{n} is a unit vector normal to the boundary $y = g(x)$.

III. METHODS OF SOLUTION

Analytical solution of the stated boundary value problem is well nigh impossible, except in a perturbative sense. Early numerical techniques [16] relied on the so-called Rayleigh hypothesis, according to which the expansions (3) can be assumed valid at $y = g(x) \pm$ [17]. Therefore, those techniques were not applicable for deeply corrugated boundaries [13]. The limitations of the Rayleigh hypothesis were overcome by the T-matrix method [8, 18] and the C formalism [19, 20], of which the latter displays superior performance. All of these techniques require various degrees of computational proficiency, and so we applied three different methods of solution for NPV diffraction gratings — as checks on each other, as applicable.

(a) Rayleigh-hypothesis method

This method was enunciated by Rayleigh [17] for gratings made by sinusoidally corrugating a perfectly reflecting sheet. According to his hypothesis, the expansions (3) have to be used in the boundary conditions (7). Both resulting equations are then projected into the Rayleigh basis $\{\exp(i\alpha_m x)\}_{m=-\infty}^{+\infty}$, in order to obtain a linear system of equations for all $c_n^{(p)}$. The refraction coefficients $c_n^{(2)}$ are then eliminated [21, 22] to yield

$$\sum_{n=-\infty}^{\infty} \frac{(1-\sigma) \left[\beta_n^{(1)} \beta_m^{(2)} + \alpha_n \alpha_m \right] - \frac{\omega^2}{c^2} [\mu_2 \epsilon_2 - \sigma]}{\beta_m^{(2)} - \beta_n^{(1)}} D_{mn} \left(\beta_n^{(1)} - \beta_m^{(2)} \right) c_n^{(1)} = \frac{(1-\sigma) \left[\beta_0^{(1)} \beta_m^{(2)} - \alpha_0 \alpha_m \right] + \frac{\omega^2}{c^2} [\mu_2 \epsilon_2 - \sigma]}{\beta_m^{(2)} + \beta_0^{(1)}} D_{m0} \left(-\beta_0^{(1)} - \beta_m^{(2)} \right) \quad (8)$$

for all m , where

$$D_{mn}(u) = \frac{1}{d} \int_0^d \exp \left[-i \frac{2\pi}{d} (m-n)x + iug(x) \right] dx. \quad (9)$$

The summation on the left side of (8) has to be appropriately truncated, and the equations are then put in the form of a matrix equation which can be solved by standard numerical methods [23].

The Rayleigh hypothesis is valid when the corrugations are not deep, and the limit of its applicability for sinusoidal gratings has been rigorously established. Millar [24] showed that the Rayleigh hypothesis is applicable for perfectly reflecting gratings of sinusoidal shape with maximum slope not exceeding 0.448. This limit was validated by Hill & Celli [25], who also noted that the methods exploiting the Rayleigh hypothesis could yield acceptable results for steeper gratings. Depine & Gigli [26] carried out detailed numerical studies to show that the Rayleigh hypothesis can be considered adequate for dielectric sinusoidal gratings with maximum slopes as high as ~ 0.92 .

(b) *Perturbative approach*

A perturbative approach applies well when the corrugations are very shallow. The integrals $D_{mn}(u)$ can be stated exactly as the power series

$$D_{mn}(u) = \sum_{j=0}^{\infty} \frac{i^j}{j!} u^j \tilde{g}^{(j)}(m-n), \quad (10)$$

where

$$\tilde{g}^{(j)}(m) = \frac{1}{d} \int_0^d [g(x)]^j \exp \left(-im \frac{2\pi}{d} x \right) dx \quad (11)$$

is the m -th Fourier coefficient of the function $[g(x)]^j$. These coefficients can be obtained through the recurrence relation

$$\tilde{g}^{(j)}(m) = \sum_n \tilde{g}^{(j-1)}(m-n) \tilde{g}^{(1)}(n), \quad j \geq 1, \quad (12)$$

beginning with

$$\tilde{g}^{(0)}(m) = \delta_{m0}, \quad (13)$$

where δ_{mn} is the Kronecker delta.

Assuming the expansion [22, 27]

$$c_n^{(1)} = \sum_{j=0}^{\infty} \frac{(-i)^j}{j!} c_n^{(1,j)}, \quad (14)$$

we arrive at an iterative scheme, whereby the coefficient $c_n^{(1,j)}$, $j \geq 1$, can be obtained in terms of all lower-order coefficients $c_n^{(1,j-1)}, \dots, c_n^{(1,0)}$ as follows:

$$c_n^{(1,j)} = \frac{1}{M_{nn}} \left\{ N_n \left[\beta_0^{(1)} + \beta_n^{(2)} \right]^j \tilde{g}^{(j)}(n) - \sum_m \left[M_{nm} \sum_{q=1}^j \binom{j}{q} \left[\beta_n^{(2)} - \beta_m^{(1)} \right]^q \tilde{g}^{(q)}(n-m) c_m^{(1,j-q)} \right] \right\}. \quad (15)$$

This scheme commences with

$$c_n^{(1,0)} = \frac{\sigma \beta_n^{(1)} - \beta_n^{(2)}}{\sigma \beta_n^{(1)} + \beta_n^{(2)}} \delta_{n0}, \quad (16)$$

which is the planewave reflection coefficient for a perfectly flat boundary (i.e., $g(x) \equiv 0$), and requires the computation of

$$N_n = \frac{(\beta_0^{(1)} \beta_n^{(2)} - \alpha_0 \alpha_n)(1 - \sigma) + \frac{\omega^2}{c^2} (\epsilon_2 \mu_2 - \sigma)}{\beta_0^{(1)} + \beta_n^{(2)}} \quad (17)$$

and

$$M_{nm} = \frac{(\beta_m^{(1)} \beta_n^{(2)} + \alpha_m \alpha_n)(1 - \sigma) - \frac{\omega^2}{c^2} (\epsilon_2 \mu_2 - \sigma)}{\beta_n^{(2)} - \beta_m^{(1)}}. \quad (18)$$

Provided the series (14) converges rapidly, the reflection coefficients $c_n^{(1)}$ can be computed quite easily even on hand-held computers.

(c) *C formalism*

In order to avoid the use of the Rayleigh expansions (3) in the corrugation region, the C formalism begins with the transformation

$$v = y - g(x). \quad (19)$$

Accordingly, the Helmholtz equations (2) change to

$$\left[\frac{\partial^2}{\partial x^2} - 2\dot{g} \frac{\partial^2}{\partial x \partial v} - \ddot{g} \frac{\partial}{\partial v} + (1 + \dot{g}^2) \frac{\partial^2}{\partial v^2} + \frac{\omega^2}{c^2} \epsilon(v) \mu(v) \right] f(x, v) = 0, \quad (20)$$

where

$$\epsilon(v) = \begin{cases} 1 \\ \epsilon_2 \end{cases}, \quad \mu(v) = \begin{cases} 1 \\ \mu_2 \end{cases}, \quad v \begin{cases} > 0 \\ < 0 \end{cases} \quad (21)$$

and

$$\dot{g} = \frac{dg}{dx}, \quad \ddot{g} = \frac{d^2g}{dx^2}. \quad (22)$$

Because the coefficients of the differential equation (20) depend on v in a piecewise fashion, the v -dependence of f is of the form $\exp(i\rho v)$ in each of the two pieces $v > 0$ and $v < 0$. Following references [20] and [28], we expressed the x -dependences of \dot{g} , f and $\partial f/\partial v$ in terms of Fourier series, and obtained the following matrix equation:

$$\left[\begin{array}{c|c} -[\mathcal{B}^{(p)}]^{-2} \left([\mathcal{A}] [\dot{\mathcal{G}}] + [\dot{\mathcal{G}}] [\mathcal{A}] \right) & [\mathcal{B}^{(p)}]^{-2} \left([\mathcal{I}] + [\dot{\mathcal{G}}] [\dot{\mathcal{G}}] \right) \\ \hline & \end{array} \right] \begin{bmatrix} [\mathcal{F}] \\ \hline [\tilde{\mathcal{F}}] \end{bmatrix} = \rho^{-1} \begin{bmatrix} [\mathcal{F}] \\ \hline [\tilde{\mathcal{F}}] \end{bmatrix}. \quad (23)$$

In this equation, $[\mathcal{A}]$ and $[\mathcal{B}^{(p)}]$ are diagonal matrixes formed by α_n and $\beta_n^{(p)}$, respectively; the (m, n) element of the Toeplitz matrix $[\dot{\mathcal{G}}]$ is the $(m - n)$ -th Fourier coefficient of \dot{g} ; $[\mathcal{O}]$ and $[\mathcal{I}]$ are, respectively, the null and the identity matrixes; while $[\mathcal{F}]$ and $[\tilde{\mathcal{F}}]$ are column vectors formed by the Fourier coefficients of f and $-i\partial f/\partial v$, respectively. Clearly, ρ^{-1} is an

eigenvalue of the 2×2 block supermatrix on the left side of (23); and the eigenvalue spectrum of this supermatrix has to be determined for the regions above ($p = 1$) and below ($p = 2$) the corrugated surface $v = 0$.

For numerical solution, the infinite system in (23) must be truncated. If only N terms are kept in each Fourier series, each block in the 2×2 block supermatrix is a $N \times N$ matrix, thus resulting in $2N$ eigenvalues for each value of p . In each region, all eigenvalues not satisfying the radiation condition at infinity should be discarded in the representation of the diffracted field. Accordingly, for $p = 1$, only those eigenvalues are acceptable for which either ρ is real-valued and positive or ρ is complex-valued with positive imaginary part [20, 28, 29]. Similarly, for $p = 2$, when the region $v < 0$ is filled with a PPV material, acceptable values of ρ must be either real-valued and negative or complex-valued with negative imaginary part. However, when the region $v < 0$ is filled with a NPV material, acceptable values of ρ must be either real-valued and positive or complex-valued with negative imaginary part. Actual diffracting materials must be dissipative; hence, whether the region $v < 0$ is occupied by a PPV or a NPV material, the criterion

$$\text{Im} [\rho] < 0 \tag{24}$$

suffices for $p = 2$. This criterion for the eigenvalues, together with the criterion (6) for selecting $\beta_n^{(2)}$, are the central modifications that we have incorporated in the conventional C formalism for making it applicable to diffraction by either PPV or NPV corrugated half-spaces.

For PPV materials, Chandezon *et al.* [29] have shown numerically and Li [30] has shown analytically that the real-valued eigenvalues and the lower-order complex-valued eigenvalues of (23) converge to $\pm\beta_n^{(2)}$ as N increases. This property must also hold for NPV materials, since, as noted by Li [20], a plane wave is an eigensolution of (2) and the transformation (19) does not change the relevant eigenvalue, whether the refracting material is of the PPV or the NPV type. Indeed, (23) indicates that when the signs of both ϵ_{2R} and μ_{2R} are changed, the eigenvalues in the refracting half-space transform into their own complex conjugates. This is demonstrated by the sample results presented in Table 1.

$c\rho/\omega$ with $N = 11$	$c\rho/\omega$ with $N = 25$	$c\beta_n^{(2)}/\omega$	n
$2.43796 \mp i0.14356$	$2.43796 \mp i0.14356$	$2.43796 \pm i0.14356$	0
$-2.43796 \pm i0.14356$	$-2.43796 \pm i0.14356$	$-2.43796 \pm i0.14356$	0
$2.11442 \mp i0.16492$	$2.10547 \mp i0.16623$	$2.10547 \pm i0.16623$	2
$-2.11442 \pm i0.16492$	$-2.10547 \pm i0.16623$	$-2.10547 \pm i0.16623$	2
$1.71339 \mp i0.20374$	$1.71413 \mp i0.20419$	$1.71413 \pm i0.20419$	3
$-1.71339 \pm i0.20374$	$-1.71413 \pm i0.20419$	$-1.71413 \pm i0.20419$	3
$0.94258 \mp i0.30709$	$1.00455 \mp i0.34841$	$1.00455 \pm i0.34841$	4
$-0.94258 \pm i0.30709$	$-1.00455 \pm i0.34841$	$-1.00455 \pm i0.34841$	4
$-1.00099 \pm i0.34382$	$-1.03946 \pm i0.33671$	$-1.03946 \pm i0.33671$	-5
$1.00099 \mp i0.34382$	$1.03946 \mp i0.33671$	$1.03946 \pm i0.33671$	-5
$1.71661 \mp i0.19773$	$1.73180 \mp i0.20210$	$1.73180 \pm i0.20210$	-4
$-1.71661 \pm i0.19773$	$-1.73180 \pm i0.20210$	$-1.73180 \pm i0.20210$	-4

Table 1: Some eigenvalues of (23) for a dielectric–magnetic material ($\epsilon_2 = \mp 6 + i0.1$, $\mu_2 = \mp 1 + i0.1$) computed for truncation parameters $N = 11$ and $N = 25$, in comparison with $\beta_n^{(2)}$, for $h/d = 0.1$, $\omega d/c = 2\pi/0.5$ and $\theta_0 = 15^\circ$. The first three columns span upgoing and downgoing waves, but only downgoing waves are acceptable in the present situation. Therefore, acceptable values of $\beta_n^{(2)}$ and ρ must conform to the restrictions (6) and (24), respectively.

Once the foregoing changes have been incorporated, implementation of the C formalism proceeds as usual. As this is well–documented in the literature [19, 20, 29], we only sketch the procedure here for completeness. The following two steps are undertaken:

(i) First, the function $f(x, y)$ is written as

$$f(x, y) = \begin{cases} f^{(1)}(x, y) \\ f^{(2)}(x, y) \end{cases}, \quad y \begin{cases} > g(x) \\ < g(x) \end{cases}. \quad (25)$$

Here, the sectional field functions

$$\begin{aligned} f^{(1)}(x, y) = & \exp \left[i (\alpha_0 x - \beta_0^{(1)} y) \right] + \sum_{n \in \mathbf{U}^{(1)}} c_n^{(1)} \exp \left[i (\alpha_n x + \beta_n^{(1)} y) \right] + \\ & \sum_m \exp(i \alpha_m x) \sum_{q \in \mathbf{V}^{(1)}} C_q^{(1)} f_{mq}^{(1)} \exp \left\{ i \rho_q^{(1)} [y - g(x)] \right\} \end{aligned} \quad (26)$$

and

$$\begin{aligned} f^{(2)}(x, y) = & \sum_{n \in \mathbf{U}^{(2)}} c_n^{(2)} \exp \left[i (\alpha_n x - \beta_n^{(2)} y) \right] + \\ & \sum_m \exp(i \alpha_m x) \sum_{q \in \mathbf{V}^{(2)}} C_q^{(2)} f_{mq}^{(2)} \exp \left\{ i \rho_q^{(2)} [y - g(x)] \right\}, \end{aligned} \quad (27)$$

contain $C_q^{(p)}$ as unknown scalars with the index q indicating the q -th eigenvalue $1/\rho_q^{(p)}$ of the 2×2 block supermatrix in (23), and $f_{mq}^{(p)}$ are the successive elements of the top half of the corresponding eigenvector. The set $\mathbf{U}^{(p)}$ contains the indexes corresponding to physically acceptable propagating plane waves, and we note that the set $\mathbf{U}^{(2)}$ is always an empty set when the refracting material is dissipative. In contrast, the set $\mathbf{V}^{(p)}$ contains indexes corresponding to physically acceptable evanescent plane waves.

(ii) Second, (26) and (27) are rewritten in terms of the variables x and v only and then introduced in the boundary conditions (7). A complete set of linear algebraic equations is thereby obtained for the sets of the unknown scalars $c_n^{(p)}$ and $C_q^{(p)}$. The $2N$ scalars are then calculated using standard methods [23].

The C formalism, not invoking the Rayleigh hypothesis and therefore not limited to gratings with shallow corrugations, is a very efficient and versatile theoretical tool for modeling the electromagnetic responses of diffraction gratings of arbitrary permittivity and corrugation shape. As stated in Ref. [28], the most distinctive feature of this formalism is its virtually uniform convergence, regardless of the incident polarization state and the permittivity of the

refracting material. Originally set up for uncoated, perfectly conducting gratings in classical mounts [19], the essence of the formalism — mainly, the simplicity of the coordinate system (19) — has allowed its extension to many other situations. Examples include multilayer-coated dielectric and metallic gratings [29], conical mountings [31], nonlinear materials [32], anisotropic materials [33, 34, 35] nonhomogeneous materials [36], and crossed gratings [37]. This versatility of the C formalism is not matched by any other rigorous method for gratings [3]. We found that the characteristic features of this formalism are valid even for diffraction gratings of isotropic NPV materials.

(d) *Conservation of energy*

Diffraction efficiencies

$$e_n^r = \frac{\operatorname{Re} [\beta_n^{(1)}]}{\beta_0^{(1)}} |c_n^{(1)}|^2, \quad (28)$$

are defined for the propagating planewave components of the reflected field in the region $y > \max g(x)$. The normalized power P_a transferred across one period of the corrugated boundary into the refracting half-space $y < g(x)$ can be calculated by virtue of the Poynting theorem, if the fields at the surface $y = g(x)$ are known. The principle of conservation of energy requires that

$$P_a + \sum_{n \in \mathcal{U}^{(1)}} e_n^r = 1, \quad (29)$$

with P_a being completely absorbed by the refracting material. When we implemented any of the methods of solution presented in Sections III(a)–(c), we checked that the condition (29) was satisfied to an error of 10 ppm.

IV. RESULTS AND CONCLUSIONS

Although corrugations of different shapes are used, we confined ourselves chiefly to the most most widely used shape:

$$g(x) = h \cos \left(\frac{2\pi x}{d} \right). \quad (30)$$

Calculations of the diffraction efficiencies were made for many values of the geometric ratio h/d and normalized periodicity $\omega d/c$, using one or all three of the methods of solution described in Section III, as applicable. These results are presented and discussed in Sections IV(a)–(c). Asymmetric counterparts

$$g(x) = h_1 \cos\left(\frac{2\pi x}{d}\right) + h_2 \cos\left(\frac{4\pi x}{d} - \gamma\right) \quad (31)$$

of the symmetric gratings (30) are addressed in Section IV(d).

(a) *Shallow gratings*

Let us begin with gratings described by (30). When the boundary $y = g(x)$ is perfectly flat, the only non-zero reflection coefficient is $c_0^{(1)}$. The transformation

$$\{\epsilon_2 \rightarrow -\epsilon_2^*, \mu_2 \rightarrow -\mu_2^*\} , \quad (32)$$

which amounts to the replacement of a NPV/PPV half-space by an analogous PPV/NPV half-space, changes the phase of $c_0^{(1)}$ but not its magnitude [10]; hence, the transformation does not affect e_0^r at all.

For a shallow grating, we therefore expect that the magnitude of the specular reflection coefficient would not be greatly affected by the transformation (32), but the effect of the transformation should be unambiguously evidenced by the nonspecular diffracted orders. This is indeed true, as was borne out by results computed using the perturbative approach of Section III(b).

Figure 2 presents the diffraction efficiencies e_0^r and e_{-1}^r as functions of $\theta_0 \in (-\pi/2, \pi/2)$ when $h/d = 0.07$ and $\omega d/c = 2\pi/0.8$. The refracting material is of either the PPV ($\epsilon_2 = 5 + i0.01$, $\mu_2 = 1 + i0.01$) or the NPV ($\epsilon_2 = -5 + i0.01$, $\mu_2 = -1 + i0.01$) type. Calculations were made for both the s - and the p -polarization cases. Two Rayleigh–Wood anomalies occur at $\theta_0 \approx 11.54^\circ$ ($\beta_1^{(1)} = 0$) and at $\theta_0 \approx 36.87^\circ$ ($\beta_{-2}^{(1)} = 0$).

Clearly, Figure 2 shows that the transformation (32) does not greatly affect e_0^r , except at low $|\theta_0|$. In contrast, the same figure shows that the nonspecular diffraction efficiency e_{-1}^r ,

which is non-zero only for $\sin \theta_0 > -0.2$, is gravely affected by the type of the refracting material.

The diversity can be understood as follows: When the boundary is perfectly flat, the transformation (32) leaves the magnitude of the reflection coefficient unchanged *only* for non-evanescent incident plane waves; but that is not a true statement for incident evanescent plane waves [38]. In the troughs of a shallow grating, i.e., for $\max g(x) > y > g(x)$, the total field actually has both specular ($n = 0$) and nonspecular ($n \neq 0$) components, by virtue of the Rayleigh hypothesis. The nonspecular components are like evanescent plane waves because they are characterized by $\text{Re} [\beta_n^{(1)}] = 0$. Their presence ensures that the nonspecular reflection efficiencies, although weak for very shallow gratings, are considerably affected — in contrast to the specular reflection efficiency — by the transformation of the refracting material from the NPV/PPV to the PPV/NPV type.

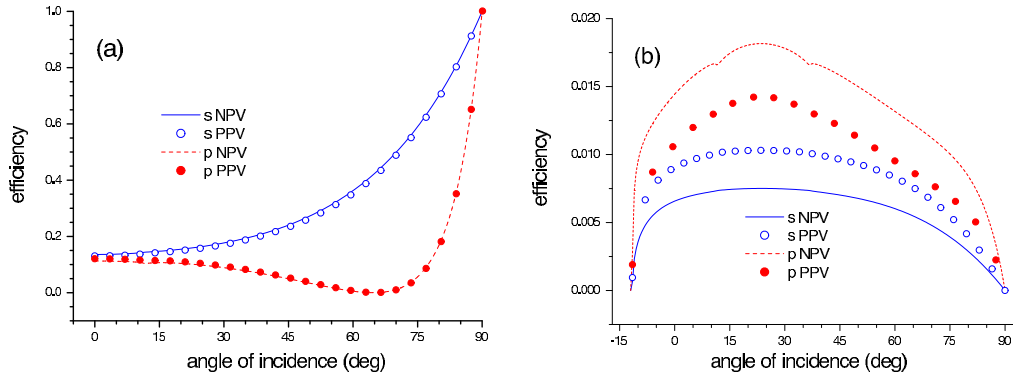


FIG. 2: Diffraction efficiencies (a) e_0^r and (b) e_{-1}^r as functions of the incidence angle θ_0 , when $h/d = 0.07$ and $\omega d/c = 2\pi/0.8$. The refracting material is of either the PPV ($\epsilon_2 = 5 + i0.01$, $\mu_2 = 1 + i0.01$) or the NPV ($\epsilon_2 = -5 + i0.01$, $\mu_2 = -1 + i0.01$) type. Calculations were made for both the s - and the p -polarization cases. Note that $e_0^r(\theta_0) = e_0^r(-\theta_0)$ and that $e_{-1}^r(\theta_0) \neq 0$ only for a limited θ_0 -range. The same results were obtained with all three methods of solution described in Sections III(a)–(c).

(b) *Deep gratings*

As the corrugations grow deeper (i.e., as h/d increases in value), the transformation of the refracting medium from NPV/PPV to PPV/NPV increasingly affects the specular efficiency e_0^r as well. This is demonstrated by the plots of the diffraction efficiencies $e_{0,-1,-2}^r$ versus θ_0 in Figure 3 for $h/d = 1$. As the Rayleigh hypothesis is inadequate for sinusoidal gratings with $h/d \gtrsim 0.3$ [34], the presented plots were obtained using the C formalism. Incidentally, Rayleigh–Wood anomalies are evident in this figure at $\theta_0 = 0^\circ$ ($\beta_{\pm 2}^{(1)} = 0$) and at $\theta_0 = 30^\circ$ ($\beta_{-3}^{(1)} = \beta_1^{(1)} = 0$).

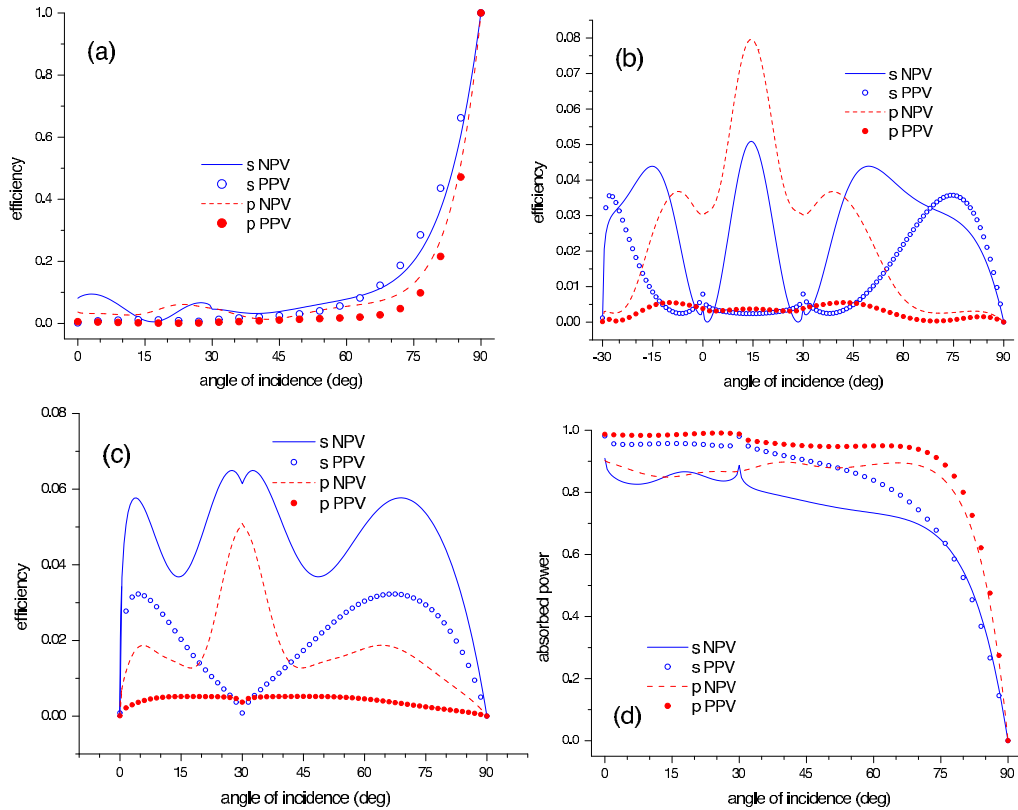


FIG. 3: Diffraction efficiencies (a) e_0^r , (b) e_{-1}^r , and (c) e_{-2}^r , and (d) normalized absorbed power P_a , as functions of the incidence angle θ_0 , when $h/d = 1$ and $\omega d/c = 2\pi/0.5$. The refracting material is of either the PPV ($\epsilon_2 = 6 + i0.01$, $\mu_2 = 1 + i0.01$) or the NPV ($\epsilon_2 = -6 + i0.01$, $\mu_2 = -1 + i0.01$) type. Calculations were made for both the s - and the p -polarization cases, using the C formalism with $N = 29$. Note that $e_0^r(\theta_0) = e_0^r(-\theta_0)$, and that $e_{-1}^r(\theta_0) \neq 0$ as well as $e_{-2}^r(\theta_0) \neq 0$ only for limited θ_0 -ranges.

(c) *Resonant surface-wave excitation*

A mechanism that can introduce dramatic changes in the diffraction efficiencies when the type of the refracting material is transformed from NPV/PPV to PPV/NPV is the resonant excitation of surface waves. Surface waves are not allowed to propagate on a plane boundary between vacuum and a material whose permittivity and permeability have positive real parts (Boardman 1982). For p -polarized (resp. s -polarized) surface waves to propagate along that boundary, the real part of the permittivity (resp. permeability) of the refracting material must be negative. Dielectric materials with negative real permittivity are exemplified by plasmas as well as metals (Boardman 1982). With the emergence of NPV materials, the propagation of both types of surface waves on the same plane boundary has become possible [39, 40], although in principle for different frequencies.

If the electromagnetic fields of the surface wave on each side of a plane boundary are described by (3) without the term corresponding to the incident plane wave and with only the $n = 0$ terms in the two series, dispersion relations can be easily obtained [39, 40]. Thus, the wavenumber α_0 of the surface wave satisfies the relation

$$\alpha_0^2 = \frac{\omega^2}{c^2} \frac{\mu_2 - \epsilon_2}{\mu_2^2 - 1} \mu_2, \quad (33)$$

for s polarization, and

$$\alpha_0^2 = \frac{\omega^2}{c^2} \frac{\epsilon_2 - \mu_2}{\epsilon_2^2 - 1} \epsilon_2, \quad (34)$$

for p polarization. These relations apply rigorously to plane boundaries only.

To illustrate how the surface wave mechanism can affect the diffraction efficiencies of a grating when the type of the refracting material is transformed from NPV/PPV to PPV/NPV, even for shallow corrugations, we performed calculations with $\epsilon_2 = -1.8 + i0.01$ and $\mu_2 = 1.5 + i0.01$. According to the conditions (1), this material is of the NPV type.

We see, from (34), that a plane boundary can support a p -polarized surface wave with $c\alpha_0/\omega \approx 1.63 + i0.01$. If the transformation (32) is implemented, the plane boundary can not support the propagation of a p -polarized surface wave; instead, as follows from (33), an s -polarized surface wave can then propagate with $c\alpha_0/\omega \approx 1.99 + i0.02$. As the real parts of

both values of $c\alpha_0/\omega$ are greater than unity, neither of the two types of surface waves can be resonantly excited by illuminating the plane boundary by a plane wave from the vacuum side.

However, as is well-established in the grating literature [41, 42], surface waves can be coupled to propagating waves through the periodicity of a corrugated boundary. If the period of the grating is conveniently chosen, the surface wave can be coupled with one of the nonspecular components (i.e., $n \neq 0$). For example, after choosing $\omega d/c = 2\pi/1.51$ and assuming that the wavenumber of the surface wave is not appreciably altered by the corrugation, (4) for α_n predicts a coupling at $\theta_0 \approx 7^\circ$, when the refracting material is of the NPV type ($\epsilon_2 = -1.8 + i0.01$, $\mu_2 = 1.5 + i0.01$). This is confirmed by the numerical results shown in Figure 4 for $h/d = 0.07$. The zeroth-order efficiency curve as a function of angle of incidence (Figure 4a) for s -polarization is almost flat, whereas for p -polarization it exhibits a pronounced dip, near an angle of incidence very close to that predicted by the quasiplane approximation (34) for surface-wave excitation. This dip, at $\theta_0 \approx 7.9^\circ$, is not related to a redistribution of the incident power between other reflected orders (i.e., a Rayleigh-Wood anomaly). Instead, this dip is associated with a peak in the power absorbed in the refracting material, as can be seen from the P_a - θ_0 curve in Figure 4b. At the dip, nearly 87% of the p -polarized incident power is absorbed by the refracting material, whereas just less than 2% of incident power is absorbed at all angles of incidence for the other polarization case.

That the transformation of the type of the refracting material from NPV to PPV radically alters the conditions for surface-wave excitation is evident on comparing Figures 4 ($\epsilon_2 = 1.8 + i0.01$, $\mu_2 = -1.5 + i0.01$) and 5 ($\epsilon_2 = -1.8 + i0.01$, $\mu_2 = 1.5 + i0.01$). Three differences are noticeable. First, the polarization-dependences are different: whereas the the NPV grating exhibits a strong absorption peak for p - but not for s -polarization, its PPV analog exhibits a strong absorption peak for s - but not for p -polarization. Second, the absorption peaks occur at different angles of incidence for the two types of materials. The peak absorption in Figure 4 occurs for p -polarization at $\theta_0 \approx 7.9^\circ$, but for s -polarization at $\theta_0 \approx 30.9^\circ$ in Figure 5b. Third, although both peak absorptions are very strong, that in Figure 5, near $\theta_0 \approx 30.9^\circ$, is almost total (nearly 99% of the s -polarized incident power).

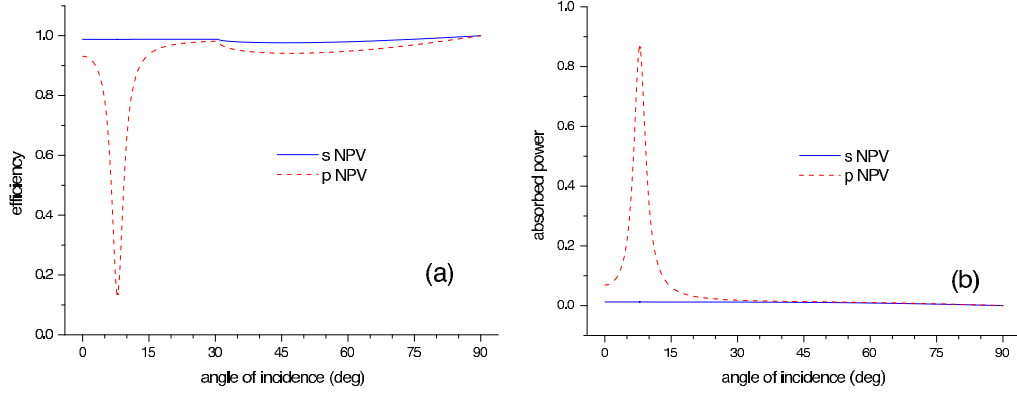


FIG. 4: (a) Diffraction efficiency e_0^r and (b) normalized absorbed power P_a functions of the incidence angle θ_0 , when $h/d = 0.07$ and $\omega d/c = 2\pi/1.51$. The refracting material is of the NPV ($\epsilon_2 = -1.8 + i0.01$, $\mu_2 = 1.5 + i0.01$) type. Calculations were made for both the s - and the p -polarization cases using all three methods presented in Section III.

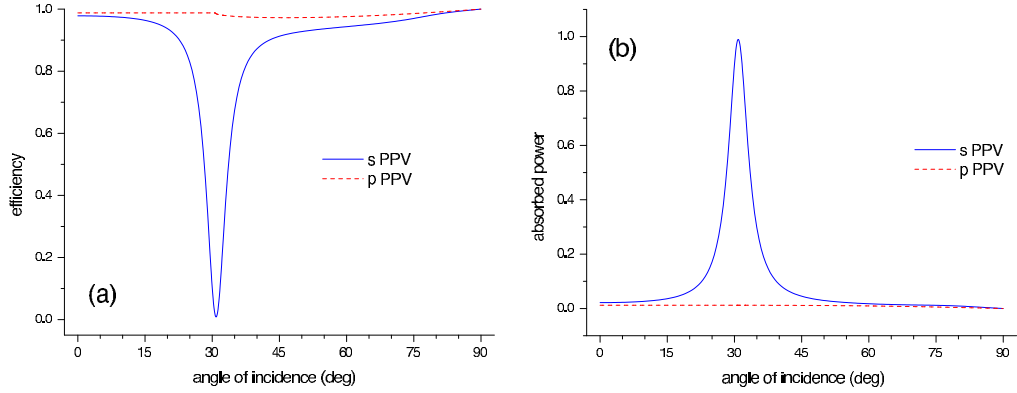


FIG. 5: Same as Figure 4, except that the refracting material is replaced by its PPV analog ($\epsilon_2 = 1.8 + i0.01$, $\mu_2 = -1.5 + i0.01$).

For gratings with deep corrugations, the wavenumber of the surface wave can be appreciably different from the values in the absence of the corrugations, or the surface wave can even be forbidden to propagate. This can be concluded from Figures 6 and Figures 7, which were drawn for the same parameters as for Figures 4 and Figures 5, except that now $h/d = 1$. Apparently, the p -polarized surface wave does still play a role in the diffraction by the NPV grating (Figure 6c), with a broad absorption peak at $\theta_0 \approx 10.5^\circ$, close to the value found for

$h/d = 0.07$ in Figure 4b. But no resonant behavior can be seen in Figure 7, the refracting material then being of the PPV type. The Rayleigh–Wood anomaly determined by $\beta_{-1}^{(1)} = 0$ is indicated in both figures at $\theta_0 \approx 30.5^\circ$.

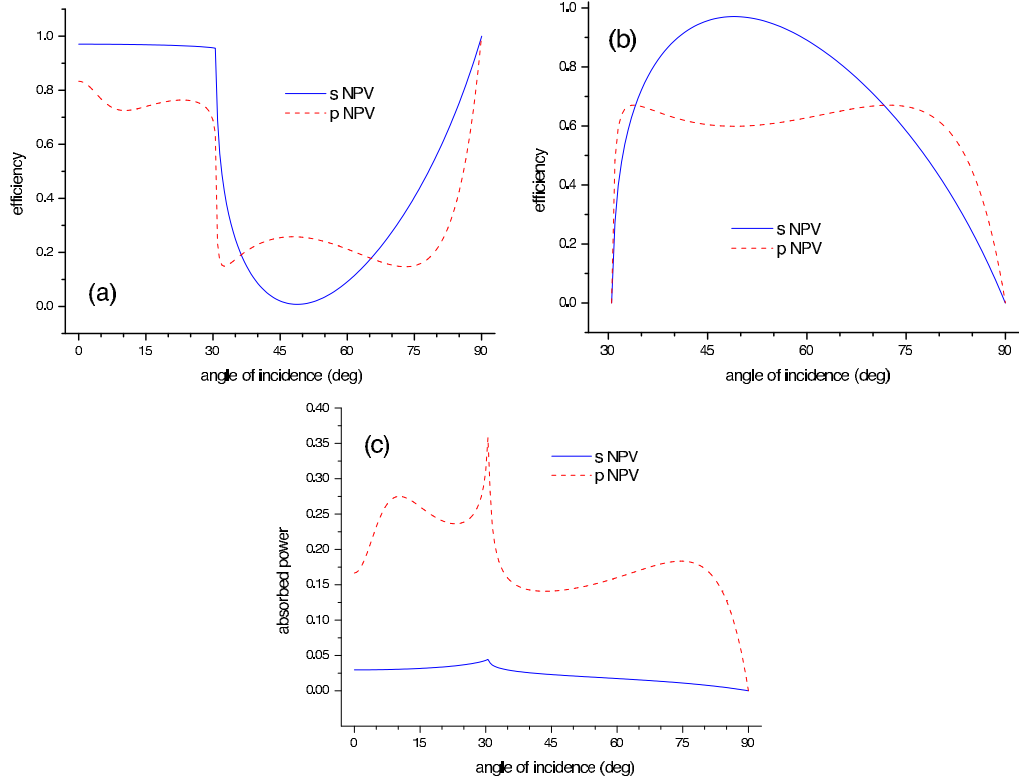


FIG. 6: Diffraction efficiencies (a) e_0^r and (b) e_{-1}^r and (c) normalized absorbed power P_a as functions of the incidence angle θ_0 , when $h/d = 1$ and $\omega d/c = 2\pi/1.51$. The refracting material is of the NPV ($\epsilon_2 = -1.8 + i0.01$, $\mu_2 = 1.5 + i0.01$) type. Calculations were made for both the s - and the p -polarization cases using the C method with $N = 29$.

(d) *Asymmetric corrugations*

In order to illustrate effect of the corrugation shape on the diffraction efficiencies, we also considered asymmetric corrugations described by (31). Diffraction efficiencies were calculated

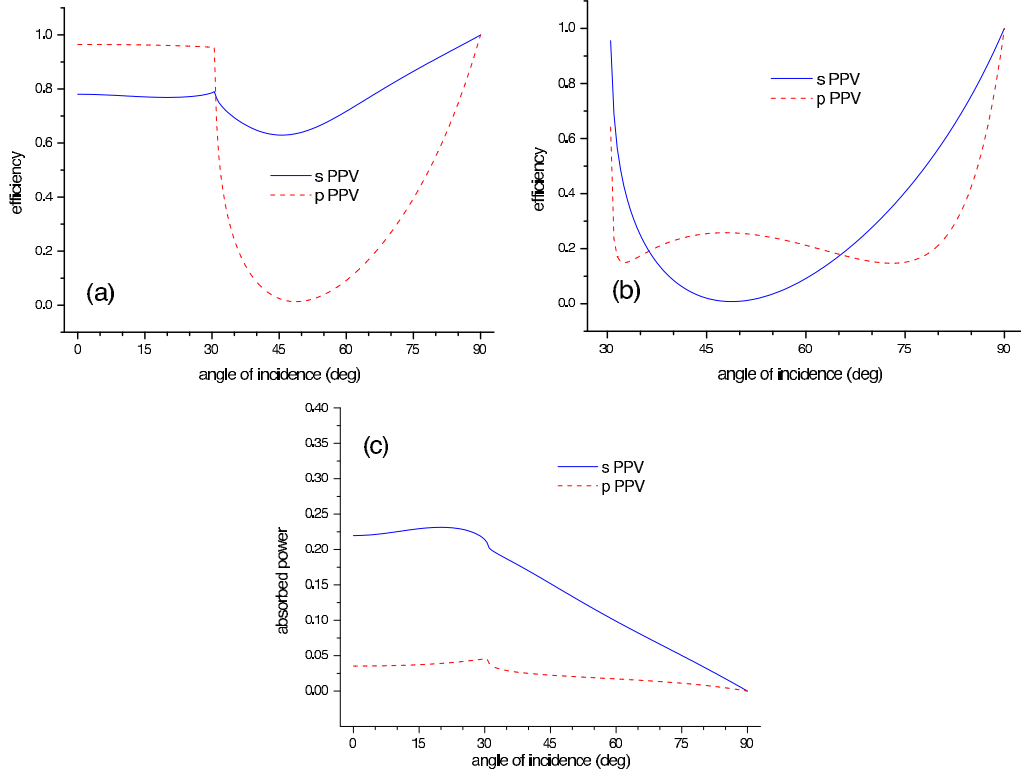


FIG. 7: Same as Figure 6, except that the refracting material is replaced by its PPV analog ($\epsilon_2 = 1.8 + i0.01$, $\mu_2 = -1.5 + i0.01$).

for $h_1/d = 0.12$, $h_2/d = 0.078$ and $\gamma = \pi/2$, so that $(\max g(x) - \min g(x))/d \simeq 0.33$. Calculated values of e_0^r , e_{-1}^r , e_{-2}^r , and P_a as functions of the incidence angle θ_0 are plotted in Figure 8 for $\omega d/c = 2\pi/0.5$, when the refracting material is of either the PPV ($\epsilon_2 = 5 + i0.01$, $\mu_2 = 1 + i0.01$) or the NPV ($\epsilon_2 = -5 + i0.01$, $\mu_2 = -1 + i0.01$) type. These plots were made for both the s - and the p -polarization cases, using the C formalism with $N = 29$. Clearly, application of the C formalism is not limited to simple sinusoidal gratings. Additionally, as in Sections IV (a) and (b), the differences between NPV and PPV gratings are easy to divine from Figure 8, and Rayleigh–Wood anomalies are present therein.

The corrugation shape should affect surface wave propagation. This conjecture was verified when the calculations for Figures 4 ($\epsilon_2 = -1.8 + i0.01$, $\mu_2 = 1.5 + i0.01$) and 5 ($\epsilon_2 = 1.8 + i0.01$, $\mu_2 = -1.5 + i0.01$) were repeated, but for the shape delineated by (31). Figures 9 and

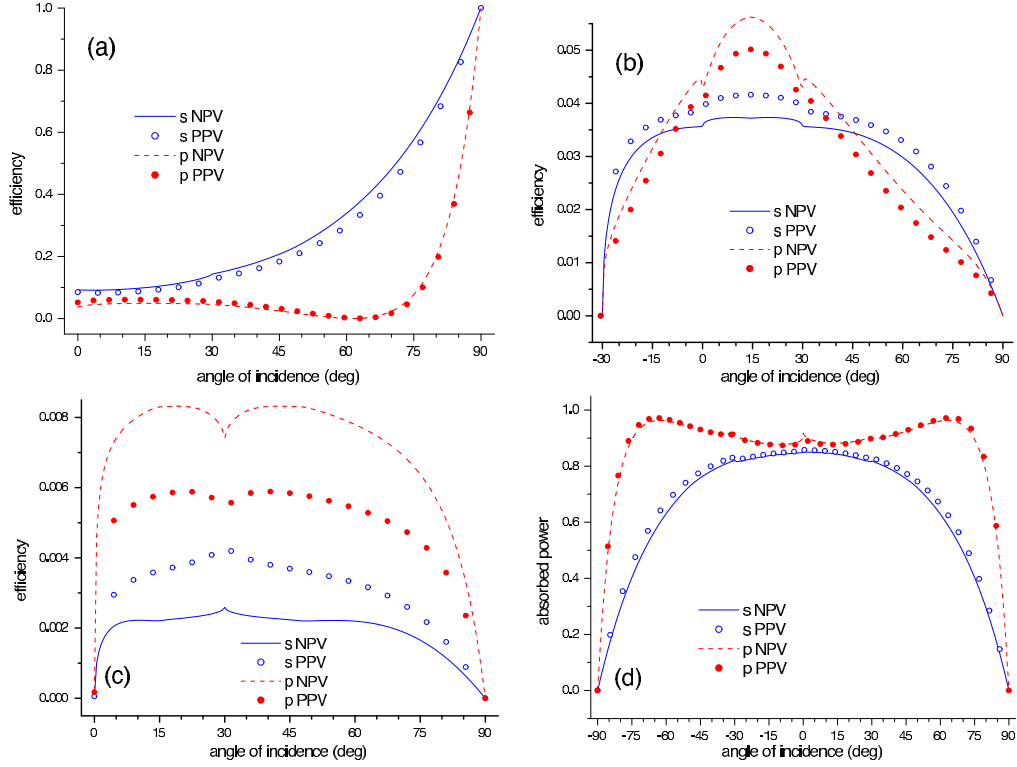


FIG. 8: Diffraction efficiencies (a) e_0^r , (b) e_{-1}^r , and (c) e_{-2}^r , and (d) normalized absorbed power P_a , as functions of the incidence angle θ_0 , when $\omega d/c = 2\pi/0.5$. The corrugation shape is given by (31), with $h_1/d = 0.12$, $h_2/d = 0.078$, and $\gamma = \pi/2$. The refracting material is of either the PPV ($\epsilon_2 = 6 + i0.01$, $\mu_2 = 1 + i0.01$) or the NPV ($\epsilon_2 = -6 + i0.01$, $\mu_2 = -1 + i0.01$) type. Calculations were made for both the s - and the p -polarization cases, using the C formalism with $N = 29$.

10 were drawn for $h_1/d = 0.04$, $h_2/d = 0.026$ and $\gamma = \pi/2$. As $(\max g(x) - \min g(x))/d \simeq 0.11$ is rather small, the wavenumber of the surface wave should be predicted reasonably well by (33) and (34). But the introduction of a Fourier harmonic to a sinusoidal corrugation seems to change strongly the coupling between the surface and incident waves, both for NPV and for PPV materials, as can be observed from Figures 9 and 10.

Finally, we must remark on a major difference and a major similarity between Figures 2–7 on the one hand and Figures 8–10 on the other. The corrugation shape is symmetric for the former set of figures, but asymmetric for the latter. We see that $P_a(\theta_0) = P_a(-\theta_0)$

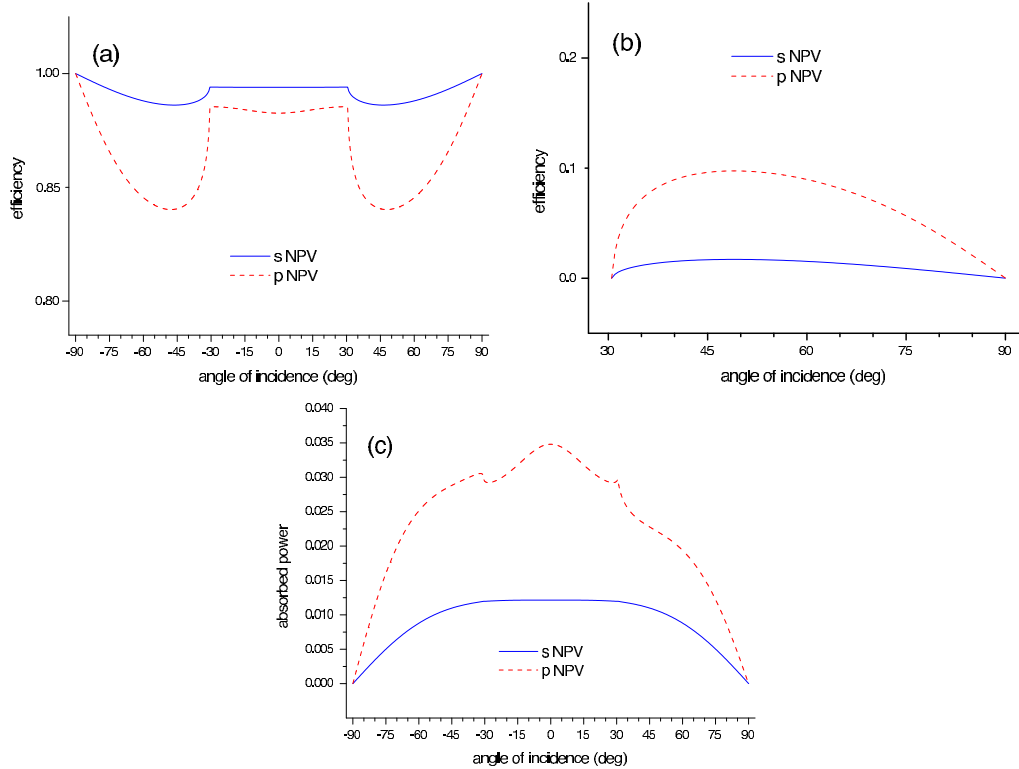


FIG. 9: Diffraction efficiencies (a) e_0^r and (b) e_{-1}^r , and (c) normalized absorbed power P_a as functions of the incidence angle θ_0 , when $\omega d/c = 2\pi/1.51$. The corrugation shape is given by (31), with $h_1/d = 0.04$, $h_2/d = 0.026$, and $\gamma = \pi/2$. The refracting material is of the NPV ($\epsilon_2 = -1.8 + i0.01$, $\mu_2 = 1.5 + i0.01$) type. Calculations were made for both the s - and the p -polarization cases, using the C formalism with $N = 29$.

for symmetric corrugations, but $P_a(\theta_0) \neq P_a(-\theta_0)$ for asymmetric corrugations. However, whether or not the corrugations are symmetric, $e_0^r(\theta_0) = e_0^r(-\theta_0)$, as expected from reciprocity arguments (Petit 1980).

V. CONCLUDING REMARKS

In the foregoing sections, we extended Rayleigh's own method, a perturbative approach, and the C formalism to encompass diffraction by surface-relief gratings made of made of

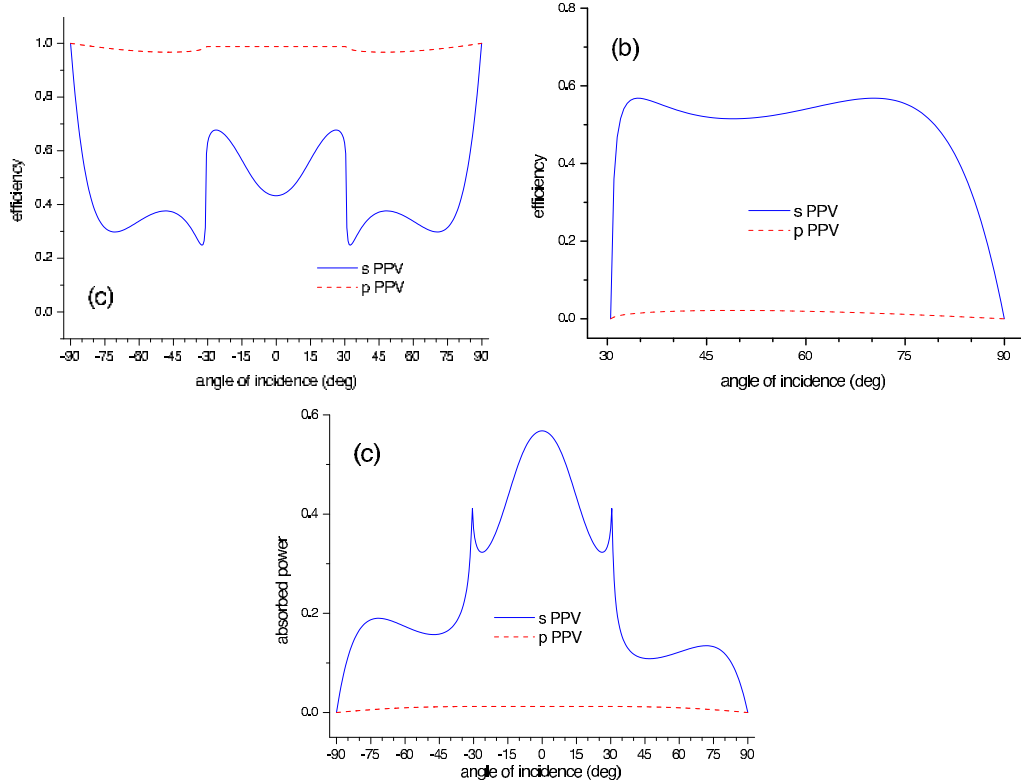


FIG. 10: Same as Figure 9, except that the refracting material is replaced by its PPV analog ($\epsilon_2 = 1.8 + i0.01$, $\mu_2 = -1.5 + i0.01$).

isotropic, negative phase-velocity materials. This was enabled by carefully representing the field inside the refracting material. Numerical results for corrugations of both symmetric as well as asymmetric shapes were obtained, as also for both s - and p -polarized incident plane waves. We concluded that replacement of a PPV grating by its NPV analog affects only nonspecular diffraction efficiencies when the corrugations are shallow. When the corrugations deepen, the specular diffraction efficiencies are also affected by the type of the refracting material.

Surface wave propagation as well as the resonant excitation of surface waves also depends on whether the refracting material is of the NPV type or its PPV analog. Excitation of a surface wave through a grating plays a fundamental role when high selectivity is desired. In common PPV gratings, surface waves have been exploited for efficient conversion of p - to

s -polarizations, or *vice versa* in conical mountings as well as to obtain enhanced nonlinear optical effects through the enhancement of surface fields usually associated with the resonant excitation of surface polaritons [41, 42]. Surface waves play an important role in the concept of a perfect lens realized using a NPV material, since the field of an image, which can not be focused by a normal lens, can be transferred through a NPV layer by the excitation of surface waves at both of its boundaries [6, 40]. We expect that NPV slabs with periodically corrugated boundaries combine both attributes.

Acknowledgments. R.A.D. acknowledges financial support from Consejo Nacional de Investigaciones Científicas y Técnicas (CONICET), Agencia Nacional de Promoción Científica y Tecnológica (ANPCYT-BID 802/OC-AR03-04457) and Universidad de Buenos Aires (UBA). A.L. acknowledges partial support from the Penn State Materials Research Science and Engineering Center.

-
- [1] A. R. Parker, 515 million years of structural colours, *J. Opt. A: Pure Appl. Opt.* **2**, R15–R28 (2000).
 - [2] G. R. Harrison, The production of diffraction gratings I. Development of the ruling art., *J. Opt. Soc. Am.* **39**, 413–426 (1949).
 - [3] D. Maystre, (ed) 1992 *Selected papers on diffraction gratings*. Bellingham, WA, USA: SPIE Optical Engineering Press.
 - [4] R. A. Shelby, D. R. Smith & S. Schultz, Experimental verification of a negative index of refraction, *Science* **292**, 77–79 (2001).
 - [5] A. Lakhtakia, M. W. McCall & W. S. Weiglhofer, Brief overview of recent developments on negative phase-velocity mediums (alias left-handed materials. *Arch. Elektron. Übertrag.* **56**, 407–410 (2002).
 - [6] J. B. Pendry (ed), Focus issue: Negative refraction and metamaterials, *Opt. Express* **11**, 639–760 (2003).
 - [7] A. Kwan, J. Dudley, & E. Lantz, Who really discovered Snell’s law?, *Physics World* **15**(4), 64

- (2002). The law of refraction can be traced back to the 10th century Iraqi scientist Ibn Sahl, and the correct spelling of *Snell's* last name is *Snel*.
- [8] A. Lakhtakia, V. V. Varadan, & V. K. Varadan, Scattering by periodic achiral–chiral interfaces, *J. Opt. Soc. Am. A* **6**, 1675–1681 (1989); corrections: **7**, 951 (1990).
- [9] M. Lester & R. A. Depine, Reflection of electromagnetic waves at the corrugated boundary between permeable dielectrics, *J. Phys. D: Appl. Phys.* **27**, 2451–2456, (1994).
- [10] A. Lakhtakia, On planewave remittances and Goos–Hänchen shifts of planar slabs with negative real permittivity and permeability, *Electromagnetics* **23**, 71–75 (2003).
- [11] R. A. Depine and A. Lakhtakia, A new condition to identify isotropic dielectric-magnetic materials displaying negative phase velocity, *Microwave and Optical Technology Letters* **41**, 315-316 (2004). <http://arXiv.org/abs/physics/0311029>
- [12] M. Born & E. Wolf, *Principles of optics, 6th ed*, Oxford, United Kingdom: Pergamon Press (1980).
- [13] P. C. Waterman, Scattering by periodic surfaces, *J. Acoust. Soc. Am.* **57**, 791–802 (1975).
- [14] C. F. Bohren & D. R. Huffman, *Absorption and scattering of light by small particles*. New York, NY, USA: Wiley (1983).
- [15] B. Y.–K. Hu, Kramers–Kronig in two lines, *Am. J. Phys.* **57**, 821 (1989).
- [16] P. M. van den Berg, Reflection by a grating: Rayleigh methods, *J. Opt. Soc. Am.* **71**, 1224–1229 (1981).
- [17] Lord Rayleigh, On the dynamical theory of gratings, *Proc. R. Soc. Lond. A* **79**, 399–416 (1907).
- [18] S.–L. Chuang & J. A. Kong, Scattering from periodic surfaces, *Proc. IEEE* **69**, 1132–1144 (1981).
- [19] J. Chandezon, D. Maystre & G. Raoult, A new theoretical method for diffraction gratings and its numerical application, *J. Opt. (Paris)* **11**, 235–241 (1980).
- [20] L. Li, J. Chandezon, G. Granet & J. Plumey, Rigorous and efficient grating–analysis method made easy for optical engineers, *Appl. Opt.* **38**, 304–313 (1999).
- [21] A. Maradudin, Interaction of surface polaritons and plasmons with surface roughness, In *Surface polaritons* (eds. V. Agranovich & D. L. Mills), Amsterdam, The Netherlands: North–Holland (1982).

- [22] M. Lester & R. A. Depine, Scattering of electromagnetic waves at the corrugated interface between index-matched media, *Opt. Commun.* **132**, 135–143 (1996).
- [23] G. Strang, *Introduction to applied mathematics*, Wellesley, MA, USA: Wellesley–Cambridge Press (1986).
- [24] R. F. Millar, On the Rayleigh assumption in scattering by a periodic surface. II, *Proc. Cambr. Philos. Soc.* **69**, 217–225 (1971).
- [25] N. R. Hill & V. Celli, Limits of convergence of the Rayleigh method for surface scattering *Phys. Rev. B* **17**, 2478–2481 (1978).
- [26] R. A. Depine & M. L. Gigli, Diffraction from corrugated gratings made with uniaxial crystals: Rayleigh methods, *J. Modern Opt.* **41**, 695–715 (1994).
- [27] C. Lopez, F. Yndurain & N. García, Iterative series for calculating the scattering of waves from a hard corrugated surface, *Phys. Rev. B* **18**, 970–972 (1978).
- [28] L. Li, & J. Chandezon, Improvement of the coordinate transformation method for surface-relief gratings with sharp edges, *J. Opt. Soc. Am. A* **13**, 2247–2255 (1996).
- [29] J. Chandezon, M. Dupuis, G. Cornet & D. Maystre, Multicoated gratings: a differential formalism applicable in the entire optical region, *J. Opt. Soc. Am.* **72**, 839–846 (1982).
- [30] L. Li, On the matrix truncation in the modal methods of diffraction gratings, paper presented at Electromagnetic Optics, 19th Topical Meeting of the European Optical Society, Hyères, France, 7–9 September 1998.
- [31] E. Popov, & L. Mashev, Conical diffraction mounting generalization of a rigorous differential method, *J. Opt. (Paris)* **17**, 175–180 (1986).
- [32] E. Popov & M. Nevière, Surface-enhanced second harmonics generation in nonlinear corrugated dielectrics: new theoretical approaches, *J. Opt. Soc. Am. B* **11**, 1555–1564 (1994).
- [33] J. B. Harris, T. W. Preist & J. R. Sambles, Differential formalism for multilayer diffraction gratings made with uniaxial materials, *J. Opt. Soc. Am. A* **12**, 1965–1973 (1995).
- [34] M. E. Inchaussandague & R. A. Depine, Polarization conversion from diffraction gratings made of uniaxial crystals, *Phys. Rev. E* **54**, 2899–2911 (1996).
- [35] M. E. Inchaussandague & R. A. Depine, Rigorous vector theory for diffraction gratings made of biaxial crystals, *J. Modern Opt.* **44**, 1–10, (1997).

- [36] G. Granet, J. Chandezon, & O. Coudert, Extension of the C method to nonhomogeneous media: application to nonhomogeneous layers with parallel modulated faces and to inclined lamellar gratings, *J. Opt. Soc. Am. A* **14**, 1576–1582 (1997).
- [37] G. Granet, Analysis of diffraction by crossed gratings using a non-orthogonal coordinate system, *Pure Appl. Opt.* **4**, 777–793 (1995).
- [38] A. Lakhtakia, Conjugation symmetry in linear electromagnetism in extension of materials with negative real permittivity and permeability scalars, *Microw. Opt. Technol. Lett.* **40**, 160–161 (2004).
- [39] R. Ruppin, Surface polaritons of a left-handed medium, *Phys. Lett. A* **277**, 61–64 (2000).
- [40] I. Shadrivov, A. Sukhorukov, Y. Kivshar, A. Zharov, A. Boardman & P. Egan, Nonlinear surface waves in left-handed materials, *Phys. Rev. E* **69**, 0166171–9 (2004).
- [41] A. D. Boardman (ed.) *Electromagnetic surface modes*, New York, NY, USA: Wiley (1982).
- [42] H. Raether, *Surface plasmons on smooth and rough surfaces and on gratings*, Heidelberg, Germany: Springer (1988).